Adv. Space Res. Vol.5, No.9, pp.129–132, 1985
Printed in Great Britain.

0273-1177/85 $0.00 + .50
COSPAR

THE PIONEER VENUS ORBITER ULTRAVIOLET SPECTROMETER EXPERIMENT: ANALYSIS OF HYDROGEN LYMAN ALPHA DATA

L. J. Paxton,* D. E. Anderson, Jr* and
A. I. F. Stewart**

**E. O. Hulburt Center for Space Research, Naval Research Laboratory, Washington, DC 20375, U.S.A.*
***Laboratory for Atmospheric and Space Physics, University of Colorado, Boulder, CO 30309, U.S.A.*

ABSTRACT

Pioneer Venus Orbiter Ultraviolet Spectrometer (PVOUVS) HI 1216Å data from six (6) orbits are analyzed. Analysis of subsolar region periapsis data show that for an exobase temperature of 305K, the exobase density is 5 ± 2(4) @ cm^{-3} and the column abundance of atomic hydrogen between 110 and 200 km is 2.4 ± 0.8(13) cm^{-2}. The upward flux through the exobase is determined to be 7.5 ± 2.5(7)/cm^2s. Apoapsis data were analyzed for both evening and morning geometries. We conclude: (1) the observed limb profiles show a diurnal variation consistent with Brinton et al. /1/; (2) the model temperature field /2/ provides a good fit to the morning data, but the morning temperature field must be used to match the evening data; and (3) the theoretical Ly α limb intensity profiles are sensitive to small changes in the shape and magnitude of the variation of exobase hydrogen with solar zenith angle. The solar Ly α flux at line center required to fit the magnitude of the data is 8(11) photons/cm^2s Å at Venus.

INTRODUCTION

The first report of the the HI 1216Å Lyman- α airglow emission from the Venus hydrogen (H) corona was published nearly twenty years ago /3/. The history of these observations has been reviewed /4/. During the Pioneer Venus mission large temperature gradients were observed as function of altitude and solar zenith angle θ_o. This observation stimulated the development of a more detailed radiative transport model which properly describes the radiation field when the density and temperature fields vary with altitude, latitude, and local time. Although this increases the dimension of the parameter space to be investigated, empirical models /2/ provide guidelines for the horizontal and vertical temperature profiles. The analysis described here attempts to answer specific questions regarding the H distribution, rather than to provide a detailed description of the global H distribution. What is the atomic hydrogen column density between 110 and the exobase? Are hydrogen densities deduced from neutral and ion mass spectrometer data /1/, consistent with the PVOUVS Lyman- α observations? Is it possible to globally determine the exobase density and fluxes by remote sensing?

THEORETICAL MODELS

Hydrogen Distribution

The vertical distribution of the atomic hydrogen above the exobase is calculated using the Chamberlain model /9/. In the radiative transfer calculations, the H distribution is taken as the sum of the thermal and non-thermal distribution, while the temperature above the critical level is modelled as the density weighted average of the thermal and hot components. Our analysis is relatively insensitive to the details of the temperature profile and line shape of the hot exospheric component.

In the absence of photochemistry, the H distribution between 110 km and the exobase Z_c =200 km can be approximated by solution of the diffusion equation with eddy diffusion and H escape flux (eqn. 13 of /11/). The recent interpretation of the mass 2 peak in the ion mass spectrometer data as deuterium /10/ essentially eliminates the H_2 photochemistry in the thermosphere as an important source of H atoms. Below 110 km, pure absorption by CO_2 extinguishes Lyman- α radiation.

@ read 5(4) as 5×10^4

Radiative Transfer Model

The vertical optical depth in hydrogen above 110 km on Venus is in the range 1-100. The exact value depends on the solar zenith angle, the escape flux of H and perhaps the solar cycle. Suggested horizontal gradients in exobase temperature T_c /5, 6/ have been confirmed by Pioneer Venus mass spectrometer data (/2/ and refefences cited therein). The H density at the exobase N_c varies by as much as a factor of 300 from day to night /1/.

Such large temperature and density gradients preclude the use of isothermal, spherically symmetric models (e.g. /6, 8, 12/) except as a first approximation to the hydrogen density distribution. The radiative transfer model developed by Anderson and Hord /7/ for an isothermal spherically symmetric atmosphere has been extended to include temperature dependent scattering /13, 14/ and to accommodate [H], [CO_2], and T variations with altitude, latitude, and local time. Isothermal models of geocoronal Lyman- α have been shown to be in error by nearly a factor of 2 /15, 16/.

DATA ANALYSIS

Six orbits were chosen for this analysis: three orbits which provided periapsis data in the subsolar regions, and three orbits for which apoapsis scans were obtained of the morning terminator, the evening terminator, and the subsolar region. Periapsis data were taken at 32 ms integration period; for the apoapsis data, 8 ms and 16 ms were utilized. The apoapsis data were chosen so that the PVOUVS slit was oriented perpendicular to the limbs, with a projected field of view of less than 100 km when the spacecraft is 20,000 km above Venus, obviating field of view averaging. The design and operation of the PVOUVS have been discussed /17/. A line center solar Lyman- α flux of 8.0(11) photons/cm^2-s-Å at Venus is used in the intensity calculations. A two year average of the line center flux based on the F10.7 radio flux, the relation of solar Lyman- α flux to line center solar flux and empirical formulae /18/ relating total solar Lyman- α flux to the F10.7 cm flux yields a value of 7.8(11) photons/cm^2-s-Å.

Periapsis Data. Periapsis data and theoretical models for orbit 190 are shown in Figure 1a and 1b. The dependence of the shape and magnitude of the intensity on the atomic hydrogen escape flux F_c are demonstrated in Figure 1a; while changes in the calculated intensity due to the variation of N_c are shown in Figure 1b. The periapsis data are clearly sensitive to changes in both N_c and F_c. The dashed curve in Figure 1b fits the data near the limb, but falls significantly below the data when viewing the nadir. Doubling N_c improves the nadir profile, but the theoretical intensity at the limb is then much too high. The best fit to the data shown in Figure 1a required varying both N_c and F_c until a satisfactory fit was obtained; N_c = 5(4)/cm^3 and F_c = 7.5(7)/cm^2-s. Analysis of orbit 198 produced results consistent with these result, whereas orbit 405 suggested that F_c = 5(7) /cm^2-s provided a better fit to the data. This analysis indicates that a systematic analysis of periapsis data as a function of θ_o can yield an accurate description of the variation of N_c and F_c with solar zenith angle.

Apoapsis Data. Analysis of apoapsis data is more complex. Contributions to the limb intensity from a range of θ_o along the line of sight preclude the use of symmetric models, except for qualitative estimates of trends in the data. Apoapsis data for orbits 119 and 238 are shown in Figure 2. The spacecraft solar zenith angle was near 90° for both orbits; the PVOUVS viewed the evening terminator on orbit 119 and the morning terminator during orbit 238. Although an exhaustive study with symmetric models was not carried out, over two dozen combinations of N_c and F_c failed to fit either the morning or evening data. The morning terminator data are represented by the triangles, and the solid curves passing through these data in Figure 2 represent the intensity calculated with F_c = 7.5(7)/cm^2 - s, and the morningside temperature field /2/. The variation of N_c with θ_o used in the calculation is compared in Figure 3 to the values deduced by/1/. It was found that small changes in the slope and magnitude of the variation of N_c with θ_o were reproduced in the variation of intensity with θ_o; thus, the differences are both real and significant.

The evening terminator data from orbit 119, represented as +'s in Figure 2, were more difficult to fit than the morning data. After several attempts using the evening temperature field of /2/ and a number of different profiles of N_c with θ_o similar to the Brinton et al. /1/ model, it was determined that the fault lay with the model temperature field. Of the dozen or so models tried, only those with very low values of N_c were able to reproduce the data beyond the terminator. The amount of exospheric hydrogen may also be reduced by lowering the exobase temperature. We replaced the evening terminator temperature field with the morning temperature field of /2/. The solid curve passing through the evening data in Figure 2 represents the resultant fit obtained when the N_c versus θ_o profile represented in Figure 3 for the evening terminator is included. A clear difference between the morning and evening intensity profile exists.

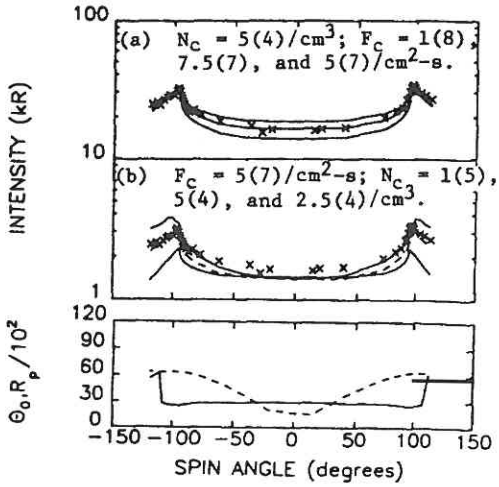

Fig. 1.
Data taken when PVO is near periapsis are compared to model for orbit 190. The upper and lower figures [(a) and (b)] differ only by a scaling factor of 10. The one sigma error bars are smaller than the X's used to indicate the data. The geometry parameters R_p (the radial distance to the minimum ray height point) and θ_o (the solar zenith angle at the minimum ray height point) are shown in the lower portion of the plot as a dashed and solid line, respectively. R_p has been scaled by a factor of 100.

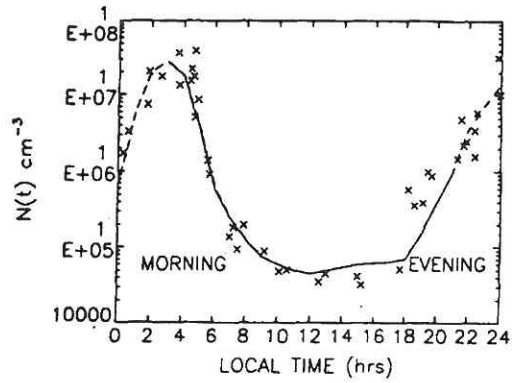

Fig. 3.
The derived distribution of the atomic hydrogen density at 165 km as a function of local time (solid line) is compared to a year's worth of in situ measurements /1/. The dashed curve represents the projected variation which is at this point largely speculative. The model is sensitive to departures of the derived density from /1/. These departures represent real and significant differences in the H mixing ratio.

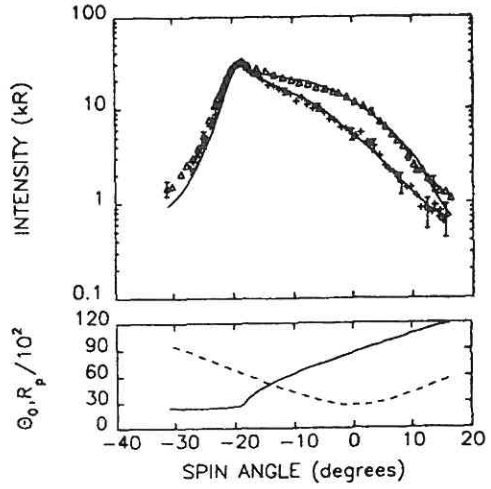

Fig. 2.
Evening and morning terminator data are compared to model calculations. The morning twilight data (triangles) are brighter than the evening twilight data (+'s) when the line of sight intersects the disk. The spacecraft altitude was 15300 km and the PVO solar zenith angle was ~90°. The geometry parameters, R_p (dashed line) and θ_o (solid line), are shown in the lower portion of the plot.

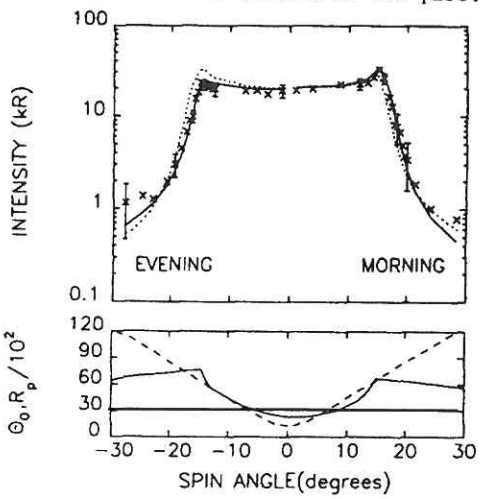

Fig. 4.
The results of a symmetric (dashed line) and assymetric (solid line - see Figure 3) model compared to subsolar region data from orbit 517. The error bars are three sigma deviations. While a symmetric model can provide a reasonable fit, the physics of the atmosphere is not represented. The PVO was at 21,200 km and its solar zenith angle was 20°.
The geometric parameters for the data arc, R_p and θ_o, are shown in the lower portion of the plot as dashed and solid curves, respectively.

The apoapsis scans for orbit 517 (Figure 4) represent information about the subsolar region when viewing the disk ($\theta_o \sim 20^o$) and looking toward the evening and morning terminators. The solid curves represent the intensity calculated with the density model in Figure 3, T_c=305 K, and F_c=7.5(7)/cm^2-s. The dashed curves represents the intensity calculated when the evening and morning density distribution are exchanged. Symmetric models yield a reasonably good fit to the data. Although symmetric models can produce good results, it is striking how well the totally asymmetric model fits the data. No scaling was required.

CONCLUSIONS

Periapsis and apoapsis Lyman- α data obtained by the PVOUVS were analyzed for six orbits separated by almost two Venus years. We conclude the line center solar Lyman- α flux at Venus is 8(11) photons/cm^2-s-Å for the data analyzed. Analysis of periapsis data at low solar zenith angles shows that the column abundance and the value of exobase density between 110 and 200 km can be determined to within $\pm$ 30%. We find $N_c = 5 \pm 2(4)$ cm^{-3} and a column abundance equal to $2.4 \pm 0.8(13)$ cm^{-2}. The column abundance of hydrogen may vary with time and solar zenith angle; however, a comprehensive examination of the PVOUVS data base is required to quantify this statement. Exobase densities derived from both periapsis and apoapsis data are consistent with the morning-evening, day-night hydrogen density asymmetry observed by Brinton et al. /1/ to solar zenith angles as large as $\theta_o \sim 120^o$.

Although symmetric models can be found which provide qualitatively good fits to the data in the subsolar region, they do not represent the physical conditions in the Venus thermosphere. Single scans from high altitude, or "fly-by" observations such as those obtained by Mariners 5 and 10 and the Veneras 8, 9, 11, and 12, do not provide enough constraints to uniquely determine the hydrogen distribution on Venus. A technique for determining the global distribution of atomic hydrogen in the exosphere and thermosphere has been demonstrated. While these results are consistent with those obtained by independent means /1/, it is important to note that only UV remote sensing continues to yield this information as periapsis rises into the exosphere. The global distribution rather than the in situ density is determined. Furthermore UV remote sensing provides the only means of obtaining a global measure of the flux of atomic hydrogen thru the exobase and the distribution of H down to 110 km.

REFERENCES

1. H. C. Brinton, H. A. Taylor, Jr., H.B. Niemann, H.G. Mayr, A.F. Nagy, T.C. Cravens, and D.F. Strobel, Geophys. Res. Lett. 7, 865, (1980)
2. A. E. Hedin, H.B. Niemann, W.T. Kasprzak, and A. Seiff, J. Geophys. Res., 88 73, (1983)
3. C. A. Barth, J. B. Pearce, K.K. Kelly, L. Wallace, and W.G. Fastie, Science 158, 1675 (1967)
4. D.E. Anderson, Jr., L.J. Paxton, and A.I.F. Stewart, submitted to J. Geophys. Res. (1984)
5. D. E. Anderson, Jr., in "The Atmosphere of Venus: Proceedings of a conference held at Goddard Institute for Space Studies Oct 15-17, 1974, ed. J.E. Hansen, p. 158
6. D. E. Anderson, Jr., J. Geophys. Res. 81, 1213, (1976)
7. D. E. Anderson, Jr., and C.W. Hord, Planet. Space Sci. 25, 563, (1977)
8. J. L. Bertaux, J.E. Blamont, M. Marcelin, V.G. Kurt, N.N. Romanova, and A.S. Smirnov, Planet. Space Sci. 26, 817, (1978)
9. J. W. Chamberlain, Planet. Space Sci. 11, 910, (1963)
10. T. M. Donahue, J.H. Hoffman, R.R. Hodges, Jr., and A.J. Watson, Science 216, 630, (1982)
11. T. M. Donahue, J. Geophys. Res. 74, 1128, (1969)
12. J. L. Bertaux, V.M. Lepine, V.G. Kurt, and A.S. Smirnov, Icarus 52, 221, (1982)
13. D. J. Strickland, and D.E. Anderson, Jr., J. Geophys. Res. 78, 6491, (1973)
14. D. J. Strickland, J. Geophys. Res. 84, 5890, (1979)
15. D. E. Anderson, Jr. P. D. Feldman, E. P. Gentieu, and R. R. Meier, Geophys. Res. Lett. 7, 529 (1980)
16. D. E. Anderson, Jr., L. Paxton, R. P. McCoy, and S. Chakrabarti, EOS Trans. Am. Geophys. Soc. 64, 789, (1983)
17. A. I. F. Stewart, IEEE Trans. Geosci. Remote Sens. GE-18, 65, (1980)
18. M. Nicolet, personal communication, (1984)